Hassanen *et al. Beni-Suef Univ J Basic Appl Sci* (2024) 13:6
https://doi.org/10.1186/s43088-024-00464-2

Beni-Suef University Journal of Basic and Applied Sciences

RESEARCH **Open Access**

Phenolic-rich fraction of green tea attenuates histamine-mediated cardiopulmonary toxicity by inhibiting Cox-2/NF-κB signaling pathway and regulating oxidant/antioxidant balance

Eman I. Hassanen[1*], Shaimaa Kamel[2], Marwa Y. Issa[3], Wafaa A. Mohamed[1], Hayam A. Mansour[4] and Mahmoud A. Mahmoud[1]

Abstract

Background Histamine (HIS) has a substantial impact on the development of numerous allergic disorders including asthma. Antihistamines mostly target histamine receptor-1 alone, so it is not entirely effective in the treatment of allergic diseases. In the current investigation, we examine the growing evidence for novel therapeutic strategies that aim to treat histamine-mediated cardiopulmonary toxicity with the phenolic-rich fraction of green tea (PRFGT).

Results Our findings demonstrated that weekly ingestion of HIS to rats induced oxidant/antioxidant imbalance in both lung and heart homogenates. The histopathological examination demonstrated extensive interstitial pneumonia with progressive alveolar and bronchial damage in HIS receiving groups. Heart sections showed severe myocardial necrosis and hemorrhage. All lesions were confirmed by the immunohistochemical staining that demonstrated strong caspase-3, cyclooxygenase-2 (Cox-2), and tumor necrosis factor-α (TNF-α) protein expressions along with upregulation of the pulmonary m-RNA expression of TNF-α, nuclear factor kappa-B (NF-κB), and interleukin-1β (IL-1β) genes and cardiac levels of many apoptotic genes. Otherwise, the pretreatment of rats with PRFGT had the ability to alleviate all the aforementioned toxicological parameters and return the microscopic picture of both lung and heart sections to normal histology.

Conclusions We concluded that PRFGT's powerful antioxidant, anti-inflammatory, and anti-apoptotic properties can reduce cardiopulmonary toxicity caused by HIS. We recommended daily intake of green tea as a beverage or adding it to foods containing elevated levels of HIS to prevent its possible toxicity.

Keywords Cardiopulmonary toxicity, Green tea, Histamine, Oxidative stress, Pathology

*Correspondence:
Eman I. Hassanen
eme_amr@cu.edu.eg; eme_amr@hotmail.com
Full list of author information is available at the end of the article

1 Background

Anaphylaxis and other allergic illnesses are becoming more common everywhere, but especially in low- and middle-income nations [71]. Around 250 million individuals worldwide have food allergies, while 300 million people have asthma [70]. Additionally, several allergic disorders frequently occur in the same person at the same time. The main mediator of allergic diseases is histamine, and it performs all its functions via four G receptors but mostly via histamine 1 receptor (H1R) [52]. Histamine is widely formed in many foods and drinks such as wine, cheese, decomposed fish, and fermented cheese via decarboxylase enzyme [35, 60]. The development of many allergy illnesses is significantly enhanced by histamine and its four receptors [87]. Histamine is widely distributed across all cells and is found in significant amounts in the lungs, skin, and digestive tract [58]. Histamine is a strong inflammatory mediator that is frequently linked to anaphylatoxins, cardiovascular alterations, and potent inflammatory reactions [19].

All green plants contain polyphenols, usually in varying amounts. In numerous experimental models, green tea extract (GTE) has a potent anti-inflammatory property [74, 78, 79, 82], through inhibiting the gene levels of nuclear factor kappa-B (NF-κB) and interleukin-1β (IL-1β) [21, 50]. Another study showed that daily consumption of green tea polyphenols over 12 weeks could enhance the blood flow and oxygen supply to the skin, protecting it from UV-damaging radiation and enhancing women's overall skin quality [34]. Additionally, green tea polyphenols' capacity to chelate transition metals and quench reactive oxygen species (ROS) has been found to have substantial antioxidant activity in vitro [49]. Following chronic cerebral hypoperfusion, green tea polyphenols at dose of 400 mg/kg per day increase the spatial cognition because of their antioxidant properties [98]. The majority of the results from research on humans showed that green tea has anti-inflammatory properties that are explained by its potent antioxidant effects that scavenge ROS and finally reduces NF-κB activity [64]. Another study explained the ability of GTE to reduce doxorubicin-induced cardiotoxicity by enhancing the heart's antioxidant defenses and bringing lipid peroxidation (LPO) levels back to normal level [46]. In osteoarthritis patients, GTE is used as an additional therapy to help manage pain and improve the physical function of the knee joints [28]. Besides the antioxidant and anti-inflammatory effects of GTE, several in vitro studies investigated its potent antiallergic effect in several cell lines via binding with immunoglobulin E (IgE) [29, 97]. Some fractions of green tea including epigallocatechin gallate and gallic acid have been investigated in several in vitro studies that demonstrating their ability to reduce IgE-mediated HIS release from mast cells and human basophiles [47, 86].

However, the in vivo study regarding the antihistaminic effect of GTE or its fraction is missed, but it is particularly important to study the potential mechanism underlying those effects. Despite increasing the incidence of histamine toxicity worldwide, it is important to find available safe ways to reduce such toxicity. Therefore, our work aimed to investigate the possible protective properties of PRFGT against HIS-mediated cardiopulmonary toxicity.

2 Methods

2.1 Preparation of green tea phenolic-rich fraction

Green tea (*Camellia sinensis*) was acquired from the local market. The identity and purity of the green tea were verified by Mrs. Therese Labib, consultant at Ministry of Agriculture and the former director of El-Orman Botanic Garden. For column chromatography, silica gel 60 (pore size 60 Å, 70–230 mesh, 63–200 μm, purchased from Fluka, Sigma-Aldrich Chemicals, Germany) was utilized. All experiments were performed at room temperature. The extract acquired from 1 kg of green tea was applied onto a silica gel column (5 × 100 cm) and then was eluted with 85:15 dichloromethane/ethanol (v/v) followed by elution with 100% ethanol. The ethanol eluate was rich in polyphenolic metabolites and was evaporated under vacuum at low temperature to dryness [51]**.** The residue was then kept at − 20 °C for further analysis and biological activities.

2.2 UPLC-MS/MS identification of green tea phenolic-rich fraction

The polyphenolic-rich fraction was dispersed in HPLC grade methanol at a concentration of 100 μg/ml, after which it was filtered through a membrane disk filter (0.2 m) and subjected to LCMS analysis using a UPLC/ESI–MS system with an ACQUITY UPLC—BEH C18 (1.7 μm—2.1 × 50 mm) column from Waters Corporation. 10 μl of the sample was injected. We used solvent of water (A) and acetonitrile (B), each containing 0.1% formic acid. Stepped mobile phase extraction was planned to start at 90% A/10% B for 2 min, increase to 70% A after 5 min, 30% A after 15 min, and 10% A after 22 min, all of which were to be maintained for 3 min. After 26 min, 100% B was reached and maintained for 3 min, and after 32 min, flow rate: 0.2 ml/min., the process resumed to the original composition. The study was done in negative ionization mode using an XEVO TQD triple quadrupole mass spectrometer from Waters Corporation in Milford, Massachusetts. The mass spectrometer's cone voltage is 30 eV, the capillary voltage is 3 kV, the source temperature is 150 °C, the dissolving temperature is 440 °C, and

the flow rates for the cone gas and the desolvation gas are 900 L/h and 50 L/h, respectively. The ESI can detect mass spectra between m/z 100 and 1000. Metabolites were potentially identified by comparing the retention durations (Rt) and mass spectra of the peaks and spectra processed using Masslynx 4.1 software with the counterparts published in databases and literature.

2.3 Animals and experimental design

All treatments applied on rats were certified by the institutional animal care and use committee of Cairo University (IACUC) (approval number: 8032022402) and following the ARRIVE guidelines (PLoS Bio 8(6), e1000412, 2010).

30-Male Wistar albino rats, weighing 170 ± 10 g, were used in this study. Five rats were housed in plastic cages and received a consistent 12 h dark/light cycle for each animal in a well-ventilated environment. They had unrestricted access to tap water during the trial as well as dry commercial standard pellets to consume. They underwent acclimatization two weeks prior to the trial's start in order to protect their health. The rats were separated into 6 groups randomly, each group consisted of 5 rats, and all rats received various treatments by oral administration for 14 days. Group (1) received distilled water. Groups (2 and 3) received PRFGT at doses 100 and 200 mg/kg BWT/day, respectively. Group (4) received HIS (98%, LOBA., India) at dose 1750 mg/kg BWT/week. Groups (5 and 6) received the identified of PRFGT + HIS as before. Both dosage levels of HIS and PRFGT were chosen according to the previous studies [13, 30, 44]

2.4 Sampling

After 14 days of treatment, rats were anaesthetized by intramuscular injection of Ketamine (90 mg/kg BWT) and Xylazine (10 mg/kg BWT) and then euthanized by the cervical dislocation and samples were collected from the primary target organs (lung and heart). All samples were split into two portions: One of them was promptly preserved in 10% neutral buffered formalin for histology and immunohistochemistry, and the other was stored at -80°C until it was required for redox status assessments and molecular analysis.

2.5 Measuring the tissue content of MDA, GSH, and catalase

Known weight samples from both pulmonary and cardiac tissue were homogenized with PBS (pH 7.4) and centrifuged at ×4500*g*. For the purpose of performing certain oxidative and antioxidant indicators, the supernatant was kept at − 80 °C. We assessed malondialdehyde (MDA), reduced glutathione (GSH), and catalase (CAT) in accordance with the guidelines provided by the manufacturer's kits (Biodiagnostic Co., Cairo, Egypt).

2.6 Histopathological examination

Following the method portrayed by Bancroft and Gamble, [10], both pulmonary and cardiac tissue specimens were washed, managed using alcohol gradients and xylene, paraffinized, sectioned into 4.5 μm thick sections, and stained with hematoxylin and eosin (H&E). We used an Olympus BX43 light microscope to examine all stained sections and an Olympus DP27 camera connected to CellSens dimension software to capture images.

A classical semiquantitative grading technique was employed following the procedures explained by Passmore et al. [69] and Hassanen et al. [32] to assess the distribution and severity of the pathological alterations within lung and heart tissues. The lung was investigated for any vascular, bronchial, alveolar, and interstitial lesions including cellular degeneration, inflammatory cells infiltration, edema, hemorrhage. Meanwhile, the heart was inspected for signs of hemorrhage, vascular congestion, interstitial edema, and muscle degeneration and necrosis. The following four-point grading scale was used to rank all the pathogenic parameters. Score (0) indicates normal histology without any microscopic changes. Score (1) indicates slight changes (tissue damage (TD) less than 10%). Score (2) indicates minor changes (TD between 11 and 25%). Score (3) indicates moderate changes (TD between 26 and 50%), while (4) means severe changes (TD greater than 50%).

2.7 Immunohistochemical staining

The apoptosis marker (caspase-3) and the inflammatory markers (Cox-2 and TNF-α) were detected in either lung or heart tissue. Briefly, the deparaffinized dehydrated tissue sections were blocked using Peroxidase (Sakura BIO) and harvested with various primary antibodies (Abcam, Ltd.), followed by reagents involved in the avidin–biotin detection system (Power Stain 1.0 Poly HRP DAB Kit; Sakura). After ten minutes of treatment with 3,3′diaminobenzidine chromogen substrate, the sections were counterstained with hematoxylin and then examined using an Olympus BX43 light microscope and photographs were taken using an Olympus DP27 camera.

2.8 RT-PCR evaluation of certain genes' m-RNA levels in cardiopulmonary tissues

Lung and heart tissues weighing about 100 mg were subjected to total RNA extraction using the ABT total RNA mini extraction kit (Applied Biotechnology, co. ltd, Egypt). RNA purity and concentration were assessed using a NanoDrop ND-1000 spectrophotometer [41]. The c-DNA synthesis was performed by using ABT

H-minus c-DNA synthesis kit (Applied biotechnology, co. ltd, Egypt). The m-RNA expression levels of the studied genes were detected using fluorescence-based real-time detection method according to the protocol of ABT 2X sybr mix (Applied biotechnology, co. ltd, Egypt). Using the primer designing tool (https://www.ncbi.nlm.nih.gov/tools/primer-blast/), the real-time PCR primers were created, as shown in Table 1. Each real-time PCR was done in triplicate, and the GAPDH gene was used as internal control [4, 5, 43]. The fold change of the results was calculated from the equations of CT, ΔCT, ΔΔCT, and $2^{-\Delta\Delta CT}$ [20, 37].

2.9 Statistical analysis

The statistical package program (SPSS version 20) was used to analyze the recorded results using one-way analysis of variance (ANOVA) and post hoc Duncan's test; *P* values less than 0.05 indicate statistical significance. The parametric data were displayed as means ± standard error, while Kruskal–Wallis H test and Mann–Whitney *U* test were utilized to analyze the nonparametric results such as histopathological scoring which is represented as a median.

3 Results

3.1 UPLC-MS qualitative profiling of phenolic-rich fraction in green tea

A total of 52 metabolites were tentatively identified in the phenolic-rich fraction of green tea (Table 2, Fig. 1). All the identified compounds were mainly of phenolic nature belonging to the flavonoids group the majority of which are flavan-3-ol and flavanol derivatives, in addition to phenolic acids. Flavan-3-ols, known as monomeric flavanols, include epicatechins, epigallocatechin, and their gallate derivatives. The major flavan-3-ol identified compounds in the green tea phenolic-rich fraction 21, 35, 41, and 47 at ESI^- m/z 289^-, 577^-, 441^-, and 451^- generated a common product ion at m/z 289 which is a characteristic mass of epicatechin. These compounds were tentatively identified as epicatechin, procyanidin B, epicatechin gallate, and epicatechin-hexoxide, respectively. Compounds 12 and 44 at m/z 305^- and 457 showing the molecular ion m/z 305^- of epigallocatechin were identified as epigallocatechin and epigallocatechin gallate, respectively.

A total of 13 flavanols were tentatively identified in the phenolic-rich fraction of green tea. The major compounds 32, 37, and 40 showing product fragment ions at m/z 285 were identified as kaempferol glycosides, namely kaempferol rutinoside, kaempferol hexosyl deoxyhexosyl hexoside and kaempferol hexosyl deoxyhexosyl hexoside, respectively. In addition to, other flavanols as myricetin and quercetin derivatives were identified from their mass fragmentation and compared to the literature as depicted in Table 2.

Ten phenolic acids (5 hydroxybenzoic acids and 5 hydroxycinnamic acids and derivatives) were identified in the phenolic-rich fraction of green tea. Gallic acid was the most abundant identified phenolic acid. The removal of the CO_2 (44 Da) and hexosyl moiety (162 Da) from their parent ions serves as a common example of the MS/MS fragmentation pattern of phenolic acids. Seven organic acids were detected as denoted in Table 2, and one polyphenol, viz. theaflavin-3,3'-digallate.

3.2 Oxidative stress evaluations

HIS receiving group displayed noticeably greater levels of MDA and lower levels of GSH and CAT than other groups. On the other side, the PRFGT-treated groups at both doses displayed significantly lower MDA content

Table 1 Primers sequences used for qRT-PCR

Gene symbol	Gene description	Accession number	Primer sequence
NF-κB	Nuclear factor kappa-B	NM_001276711.1	F: 5'-CACTGTCAACAGATGGCCC-3' R: 5'-GTCTGTGAGTTGCCGGTCTC-3'
TNF-α	Tumor necrosis factor alpha	NM_012675.3	F: 5'-ACACACGAGACGCTGAAGTA-3' R: 5'-GGAACAGTCTGGGAAGCTCT-3'
IL-1β	Interleukin-1 beta	NM_031512.2	F: 5'-TTGAGTCTGCACAGTTCCCC-3' R: 5'-GTCCTGGGGAAGGCATTAGG-3'
c-Jun	c-Jun N-terminal kinases (JNKs)	NM_053829.2	F: 5'-GTCATTCTCGGCATGGGCTA -3' R: 5'-TGGACGCATCTATCACCAGC-3'
c-Fos	Fos proto-oncogene, AP-1 transcription factor subunit	NM_022197.2	F: 5'-ACGACCATGATGTTCTCGGG -3' R: 5'- GCTGTCACCGTGGGGATAAA-3'
c-Myc	c-myelocytomatosis oncogene product or MYC proto-oncogene, bHLH transcription factor	NM_012603.2	F: 5'-AGTCAGGGTCATCCCCATCA-3' R: 5'- AAAGCTACGCTTCAGCTCGT -3'
GAPDH	Glyceraldehyde3-phosphate dehydrogenase	NM_017008.4	F:-5'-ACCACAGTCCATGCCATCAC-3' R:-5'-TCCACCACCCTGTTGCTGTA-3'

Table 2 Peak assignments of metabolites in the phenolic-rich fraction of *Camellia sinensis* using UPLC-MS in negative ionization mode

Peak no	Assignment	Molecular Formula	RT (min)	Precursor ion m/z $[M-H]^-$	Product ions MS/MS	Chemical class	References
1	Malic acid	$C_4H_6O_5$	0.75	133.0137	115,113,105,89, 87,73,71,57	Organic acid	Liu et al. [54]
2	Citramalic acid/cinnamic acid	$C_5H_8O_5$	0.77	147.0267	101,85	Organic acid	Liu et al. [54]
3	Oxoadipic acid	$C_6H_8O_5$	0.79	159.0712	131,115,113,103	Organic acid	Liu et al. [54]
4	(Iso)citric acid	$C_6H_8O_7$	0.81	191.0226	173,111,87,129, 85	Organic acid	Ezzat et al. [23]
5	Quinic acid	$C_7H_{12}O_6$	0.83	191.0459	171,127,111	Organic acid	Jeszka-Skowron et al. [39]
6	Caffeoyl-hexoside	$C_{15}H_{18}O_9$	0.91	341.0954	179,161	Hydrocinnamic acid derivative	Ezzat et al. [23]
7	Quinic acid derivative	$C_{19}H_{34}O_{17}$	0.94	533.1731	191	Quinic acid derivative	Han et al. [27]
8	Gallic acid	$C_7H_6O_5$	1.03	169.0139	125,107,97,79	Hydroxybenzoic acid	Hasim Kelebek [45]
9	5-O-Galloylquinic acid (Theogallin)	$C_{14}H_{16}O_{10}$	1.05	343.1224	191,169	Hydroxybenzoic acid	Han et al. [27]
10	Itaconic acid	$C_5H_6O_4$	1.11	129.0090	85	Organic acid	Hassanen et al. [31]
11	(Epi)gallocatechin I	$C_{15}H_{14}O_7$	1.18	305.0819	179,167,137,125	Flavan-3-ol	Shevchuk et al. [80]
12	(Epi)gallocatechin II	$C_{15}H_{14}O_7$	1.56	305.0814	179,167,137,125	Flavan-3-ol	Shevchuk et al. [80]
13	*p*-Coumaroylquinic acid I	$C_{16}H_{18}O_8$	1.79	337.1488	191,163,119	Hydrocinnamic acid	Han et al. [27]
14	(Epi)catechin	$C_{15}H_{14}O_6$	1.99	289.0767	245,205	Flavan-3-ol	Kelebek [45]
15	Caffeoylquinic acid	$C_{16}H_{18}O_9$	2.06	353.1350	191,179,135	Hydrocinnamic acid derivative	Wen et al. [95]
16	Coumaroyl hexoside	$C_{15}H_{18}O_8$	2.12	325.1510	163	Hydrocinnamic acid derivative	Abu-Reidah et al. [2]
17	Isopropylmalic acid	$C_7H_{12}O_5$	2.22	175.0398	157,131,115,87	Organic acid	Liu et al. [54]
18	Hydroxybenzoic acid	$C_7H_6O_3$	2.29	137.0280	93	Hydroxybenzoic acid	Jeszka-Skowron et al. [39]
19	(Epi)catechin-(epi) catechin (Procyanidin B) I	$C_{30}H_{25}O_{12}$	2.48	577.1374	451,425,289,125	Flavan-3-ol	Abu-Reidah et al. [2]
20	Dihydroxybenzoic acid hexoside	$C_{13}H_{16}O_9$	2.85	315.0737	153,109	Hydroxybenzoic acid	Abu-Reidah et al. [2]
21	(Epi)catechin	$C_{15}H_{14}O_6$	3.24	289.0810	245,205,179,109	Flavan-3-ol	Kelebek [45]
22	*p*-Coumaroylquinic acid II	$C_{16}H_{18}O_8$	3.64	337.1298	163	Hydrocinnamic acid	Han et al. [27]
23	Kaempferol rutinoside	$C_{27}H_{30}O_{15}$	3.71	593.2367	285,447	Flavonol	Wen et al. [95]
24	Naringenin hexoside	$C_{21}H_{22}O_{10}$	3.76	433.1012	271	Flavanone	Ali et al. [4, 5
25	Myricetin galloyl hexoside	$C_{28}H_{23}O_{17}$	4.35	631.1375	479,316	Flavonol	Abu-Reidah et al. [2]
26	Dihydroxybenzoic acid	$C_7H_6O_4$	4.40	153	91,83	Hydroxybenzoic acid	Liu et al. [54]
27	(Epi)gallocatechin gallate I	$C_{22}H_{18}O_{11}$	4.97	457.0955	305,169,125	Flavan-3-ol	Wen et al. [95]
28	Epigallocatechin gallate dihydrate	$C_{22}H_{22}O_{13}$	5.04	493.0403	457,305,169,125	Flavan-3-ol	Shevchuk et al. [80]
29	Myricetin hexoside	$C_{21}H_{20}O_{13}$	5.10	479.1303	316,271	Flavonol	Shevchuk et al. [80]
30	Theaflavin	$C_{29}H_{24}O_{12}$	5.26	563.1412	473,225	Flavan-3-ol	Shevchuk et al. [80]
31	Quercetin-hexosyl-pentosyl-hexoside	$C_{33}H_{10}O_{21}$	5.43	771.0994	609,463,301	Flavonol	Han et al. [27]
32	Kaempferol rutinoside II	$C_{27}H_{30}O_{15}$	5.58	593.2497	285	Flavonol	Wen et al. [95]

Table 2 (continued)

Peak no	Assignment	Molecular Formula	RT (min)	Precursor ion m/z [M-H]⁻	Product ions MS/MS	Chemical class	References
33	Quercetin-hexosyl-pentosyl-hexoside isomer	$C_{33}H_{10}O_{21}$	5.62	771.0994	609,463,301	Flavonoid	Han et al. [27]
34	(Epi)gallocatechin gallate II	$C_{22}H_{18}O_{11}$	5.72	457.0955	305,169,125	Flavan-3-ol	Wen et al. [95]
35	(Epi)catechin-(epi) catechin (Procyanidin B) II	$C_{30}H_{26}O_{12}$	5.79	577.2106	289	Flavan-3-ol	Wen et al. [95]
36	Quercetin rutinoside	$C_{27}H_{30}O_{16}$	5.82	609.3044	301,191,107	Flavonol	Kelebek [45]
37	Kaempferol hexosyl deoxyhexosyl hexoside	$C_{33}H_{40}O_{20}$	5.85	755.2800	593, 447, 285	Flavonol	Kelebek [45]
38	Vitexin	$C_{21}H_{20}O_{10}$	5.86	431.1213	413,341,311,269	Flavone	He et al. [33]
39	Quercetin hexoside	$C_{21}H_{20}O_{12}$	5.94	463.1440	301	Flavonol	Wen et al. [95]
40	Kaempferol hexosyl deoxyhexosyl hexoside	$C_{33}H_{40}O_{20}$	6.02	755.2800	593, 447, 285	Flavonol	Kelebek [45]
41	Epicatechin gallate	$C_{22}H_{18}O_{10}$	6.17	441.1669	289, 169, 125	Flavan-3-ol	Wen et al. [95]
42	Kaempferol rutinoside III	$C_{27}H_{30}O_{15}$	6.23	593.1575	285	Flavonol	Wen et al. [95]
43	Quercetin glucuronide	$C_{21}H_{17}O_{13}$	6.27	477.0204	301	Flavonol	Abu-Reidah et al. [2]
44	(Epi)gallocatechin gallate III	$C_{22}H_{18}O_{11}$	6.36	457.1225	305,169,125	Flavan-3-ol	Wen et al. [95]
45	Kaempferol-O-hexoside	$C_{21}H_{20}O_{11}$	6.41	447.1767	283,255,147	Flavonol	Kelebek [45]
46	(Epi)catechin-3-O-(4-O-methyl) gallate	$C_{23}H_{20}O_{10}$	6.60	455.1686	289,183	Flavan-3-ol	Kelebek [45]
47	(Epi)catechin-hexoside	$C_{21}H_{24}O_{11}$	6.84	451.0646	289	Flavan-3-ol	Liu et al. [54]
48	Kaempferol-O-trihexosyl-pentoside	$C_{38}H_{47}O_{24}$	7.19	887.2621	285	Flavonol	Abu-Reidah et al. [1]
49	(Epi)gallocatechin gallate dihydrate II	$C_{22}H_{22}O_{13}$	8.15	493.0708	457,305,169,125	Flavan-3-ol	Shevchuk et al. [80]
50	Hydroxy-octadecatrienoic acid	$C_{18}H_{30}O_3$	11.59	293.2600	221,192,71	Fatty acid	Liu et al. [54]
51	Hydroxyoctadecenoic acid	$C_{18}H_{34}O_3$	14.21	297.115	279,183,155	Fatty acid	Liu et al. [54]
52	Theaflavin-3,3′-digallate	$C_{43}H_{32}O_{20}$	14.69	867.3915	563,545,527,501,407	Polyphenol	He et al. [33]

and higher CAT and GSH content than HIS receiving group, whereas the marked improvement noticed in group receiving PRFGT at dosage level 200 mg/kg Bwt. There was no discernible difference between the HIS + high dose of PRFGT group and the control group in terms of oxidant or antioxidant levels (Fig. 2).

3.3 Histopathological examination

Compared to the control group (Fig. 3a), lung sections of HIS group displayed severe histological changes. Extremely vascular congestion accompanied by severe interstitial pneumonia was the prominent lesion in all sections. The majority of the blood vessels showed vasculitis manifested by endothelial necrosis and vascular wall thickening with inflammatory cells infiltration within and around the blood vessels (Fig. 3b). Most alveoli showed damage and others showed hemorrhage. Macrophages and eosinophils were the most noticeable inflammatory cells, along with other granulocytic cells (Fig. 3c). Moreover, there are extreme interstitial fluid and hemorrhages. The majority of the bronchi displayed epithelial desquamation, along with luminal inflammatory cells

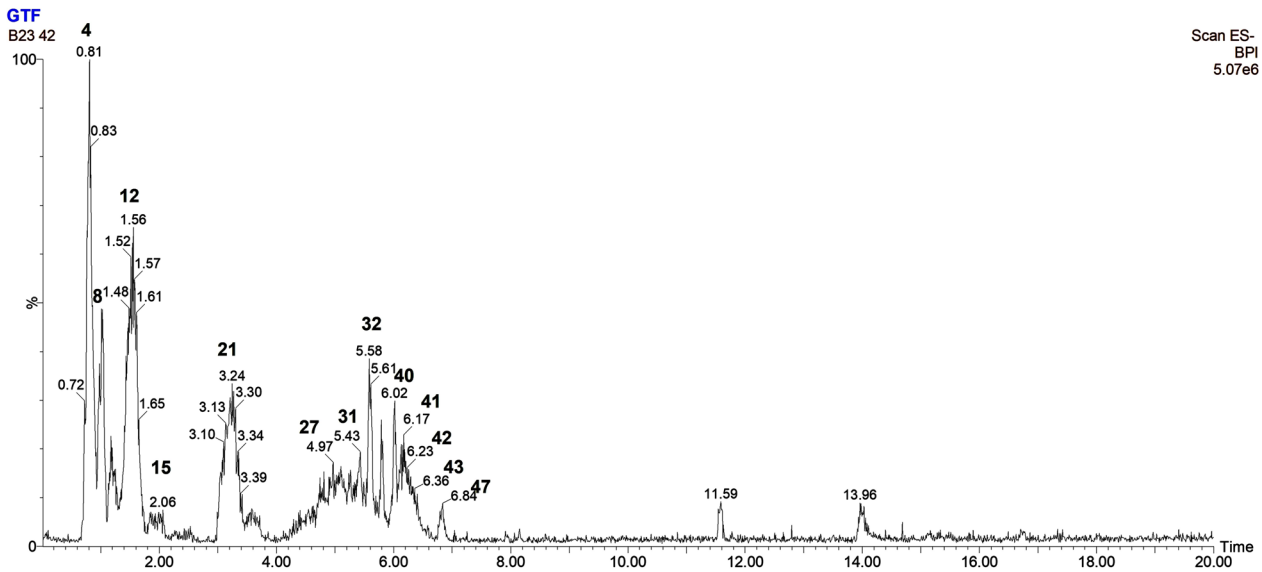

Fig. 1 Representative UPLC-MS base peak chromatogram of phenolic-rich fraction of *Camellia sinensis* in negative ionization mode

infiltration (Fig. 3d). Toluidine blue staining revealed an enormous number of dark blue/purple granulocytic mast cells in several areas especially surrounding the blood vessels (Fig. 3e). On the other side, the group cotreated with PRFGT along with HIS exhibited dose-dependent improvement in the microscopic appearance of the lung sections. Groups cotreated with 100 mg PRFGT normal histological structure of alveoli, blood vessels, bronchi, and bronchioles (Fig. 3g). However, mild thickening in the interalveolar septa by inflammatory cells infiltration was recorded in some sections along with sporadic bronchial epithelial vacuolation and necrosis (Fig. 3h). Moreover, the group receiving HIS + 200 mg PRFGT showed normal histological structure as shown in the control group (Fig. 3i–j).

Table 3 provides our findings about the microscopic lesion score in lungs of diverse groups. The score for all parameters in all HIS receiving groups significantly increased in contrast to the control group. Otherwise, PRFGT-treated groups at both doses noticed a significant reduction in the pulmonary lesion scoring compared with HIS group, whereas the lowest score noticed in high-dose receiving group. In comparison with the control group, there is not a significant difference in the microscopic score of the group receiving high dose of PRFGT.

In contrast to the control groups (Fig. 4a), a significant histological change was seen in the heart sections of HIS receiving group. There were diffuse intermuscular hemorrhage and inflammatory cells infiltration commonly eosinophils, together with myocardial degeneration and necrosis (Fig. 4b, c). While group receiving HIS + PRFGT at both doses showed marked improvement in the histological appearance of cardiac muscles (Fig. 4d, e), the best improvement was observed in group receiving the high dose (Fig. 4f).

Table 4 provides the results of the myocardial lesion scoring. The HIS obtained group showed significantly higher scores than control group and PRFGT obtained groups. Moreover, the groups receiving PRFGT at both doses showed lower scores than HIS receiving group. In comparison with those receiving the greater dose of PRFGT, the higher dose group showed a lower score.

3.4 Immunohistochemical staining

Lung samples taken from the HIS given group displayed TNF-α and Cox-2 immunopositivity stronger than other groups. On the other side, HIS + PRFGT group demonstrates dose-dependent decreasing in both immunostaining reactions. The PRFGT low-dose receiving group showed mild-to-moderate immunostaining, while those receiving the high dose did not influence any immune reactions. Heart sections obtained from HIS group demonstrated strong positive casp-3 immunoexpression. The groups cotreated with HIS and PRFGT exhibited negative to weak casp-3 immunostaining (Fig. 5).

3.5 RT-PCR evaluation of certain genes' m-RNA levels in cardiopulmonary tissues

In this study, the transcript levels of some inflammation-related genes (TNF-α, NF-κB, and IL-1β) were measured in the lung of rats. The expression levels of all genes were upregulated in the HIS group. PRFGT ameliorated the inflammatory effect of HIS on the lung of rats but did not

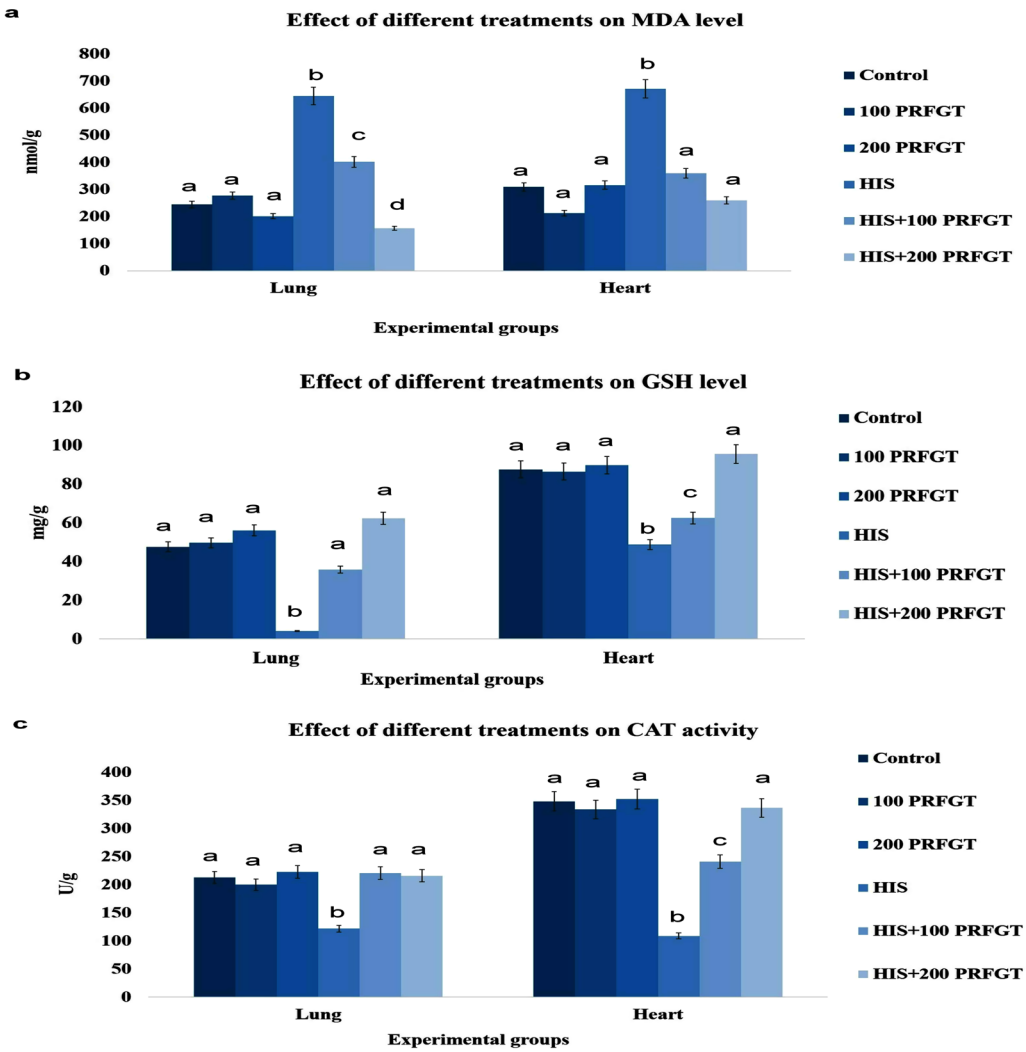

Fig. 2 Bar graphs demonstrating the effects of HIS on various oxidant and antioxidant markers in the homogenates of cardiopulmonary tissue. **a** Malondialdehyde (MDA), **b** reduced glutathione (GSH), and **c** catalase activity. Means ± SEM are used to represent values ($n = 5$). Various superscript letters (a, b, c, etc.) indicate a significant difference between groups at $P \leq 0.05$

return to the level of the control group. The higher dose of PRFGT was more effective than the lower dose. Also, three apoptosis-related genes (c-Jun, c-Fos, and c-Myc) were measured in the heart of rats. The expression levels of the apoptosis-related genes were upregulated in the HIS group. PRFGT amended the apoptotic effect of HIS on the heart of rats but did not return to the control group level. The higher dose of PRFGT was more effective than the lower dose (Fig. 6).

4 Discussion

Histamine is a biogenic amine produced from the amino acid L-histidine by the enzyme L-histidine decarboxylase and is degraded by the enzyme diamine oxidase (DAO) and histamine N-methyltransferase (HNMT) [81]. Despite the presence of both enzymes in the intestinal epithelium, DAO serves as the primary barrier of HIS absorption into the blood stream [76]. The ability of HNMT to breakdown HIS only exists intracellular, where it is found in the cytosol [68]. Several kinds of foods and drinks contain prominent levels of HIS, including wine, cheese, fermented meat, sea food, and any decomposed fish [35]. By consuming high quantities of such foods, DAO and HNMT enzyme's capacity to degrade HIS is limited, allowing it to enter the bloodstream and distribute in several organs [17]. It is distributed throughout the entire body, but lungs, skin, and digestive tract have the highest quantities [24]. Moreover, some people suffer from decreased ability of the gut to break down histamine due to diminished

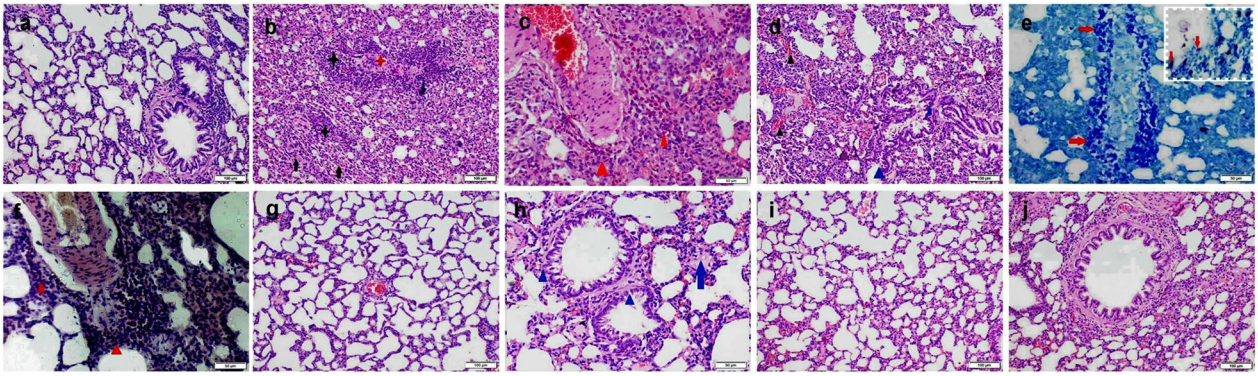

Fig. 3 Photomicrograph of lung tissue sections representing; **a** control group with normal histologic structure, **b**–**f** group receiving HIS, **g**–**h** group receiving HIS + 100 mg PRFGT, and **i**–**j** group receiving HIS + 200 mg PRFGT. Note: multifocal inflammatory cells infiltration (black stars), vasculitis (red stars), alveolar damage (black arrows), eosinophils infiltration (red triangles) bronchiolar epithelial necrosis (blue triangles) with luminal inflammatory cells infiltration (blue stars), interstitial hemorrhage (black triangles), mast cells aggregation (red arrows), and mild thickening of the interalveolar septa (blue arrows). All sections were stained with H&E except **e** stained with toluidine blue and **f** stained with Congo red

Table 3 Pulmonary lesion scoring in different treatment groups

	Control	100 PRFGT	200 PRFGT	HIS	HIS + 100 PRFGT	HIS + 200 PRFGT
Bronchial and bronchiolar lesions						
Epithelial degeneration and necrosis	0^a	0^a	0^a	2^b	0^a	0^a
Luminal inflammation	0^a	0^a	0^a	4^b	0^a	0^a
Vascular lesions						
Congestion	0^a	0^a	0^a	4^b	1^c	0^a
Perivascular inflammation	0^a	0^a	0^a	2^b	1^c	0^a
Interstitial lesions						
Inflammation	0^a	0^a	0^a	4^b	2^c	0^a
Hemorrhage	0^a	0^a	0^a	3^b	2^c	0^a
Alveolar lesions						
Collapse	0^a	0^a	0^a	3^b	1^c	0^a
Damage	0^a	0^a	0^a	3^b	1^c	0^a
Hemorrhage	0^a	0^a	0^a	3^b	2^c	0^a
Widening of alveolar septa	0^a	0^a	0^a	4^b	2^c	0^a

Data were signified as median ($n = 25$ microscopic fields). Various superscript letters (a, b, c, etc.) indicate a significant difference between groups at $P \leq 0.05$

DAO activity, which causes an accumulation of HIS in the plasma and this condition known as histamine intolerance (HIT) [17]. Histamine participates in several immunological and physiological functions as well as promoting gastric secretion, inflammation, contraction of smooth muscles, vasodilatation, permeability, and many other pathological conditions [96]. By increasing the incidence of food poisoning by HIS, it is important to find safe ways to prevent the risk of HIS poisoning in humans and animals. In our previous study, we explored the potential mechanism of repeated oral intake of HIS to rats. Thus, the current study was designed to assess the cardiopulmonary protective effect of PRFGT against such toxicity with comprehensive insight on the molecular mechanism.

Cardiac and pulmonary tissues of all HIS receiving groups displayed a discernible raise in MDA content and a decline in CAT and GSH content, indicating the presence of oxidative stress. Reactive oxygen species (ROS) overproduction is the outcome of a redux status imbalance, resulting in significant tissue damage [90]. Our histopathological outcomes revealed severe pulmonary interstitial inflammation along with myocardial degeneration because of oxidative stress. Histamine causes airway epithelial cells to produce more H_2O_2 via signaling the H1R. The main generators of ROS are Duox1 and 2

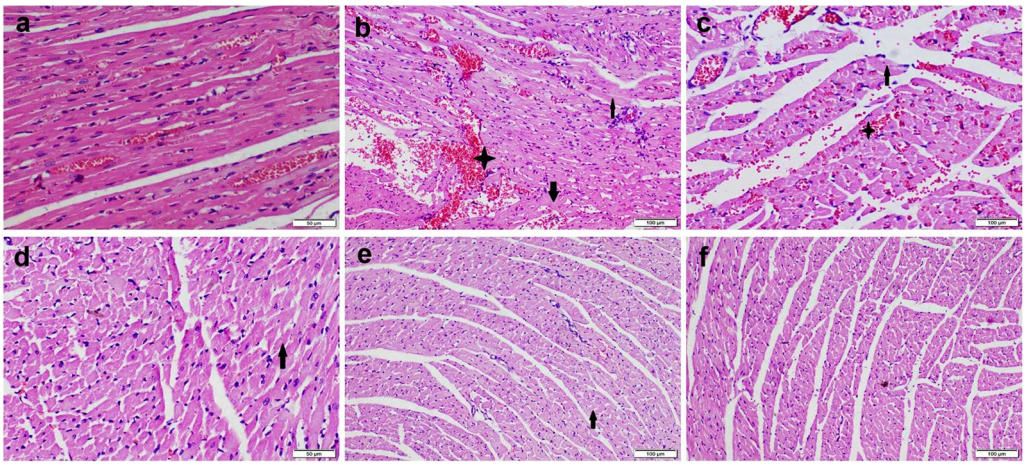

Fig. 4 H&E-stained heart tissue sections corresponding to; **a** control group with normal histological organization, **b**, **c** group receiving HIS, **d**, **e** group receiving HIS + 100 mg PRFGT, and **f** group receiving HIS + 200 mg PRFGT. Note: muscular hemorrhage (black stars), degeneration and necrosis of the myocardium (black arrows)

Table 4 Myocardial lesion scoring in different treatment groups

	Control	100 PRFGT	200 PRFGT	HIS	HIS + 100 PRFGT	HIS + 200 PRFGT
Degeneration	0^a	0^a	0^a	4^b	1^c	0^a
Necrosis	0^a	0^a	0^a	4^b	1^c	0^a
Edema	0^a	0^a	0^a	2^b	0^a	0^a
Hemorrhage	0^a	0^a	0^a	4^b	2^c	0^a

Data were signified as median ($n = 25$ microscopic fields). Various superscript letters (a, b, c, etc.) indicate a significant difference between groups at $P \leq 0.05$

that are expressed in the bronchial epithelial cells [12]. These cells have the highest amounts of H1R expression, which regulates histamine's capacity to generate H_2O_2. Inflammatory cells like neutrophils and macrophages are released when histamine is present leading to excessive ROS generation [18]. Furthermore, our results proved that mast cells and eosinophils have important roles in HIS-inducing pulmonary inflammation and cellular damage. Toluidine blue is a metachromatic stain that was largely used to identify mast cells [7], while the Congo red stain accurately diagnoses eosinophils within tissues [73]. Mast cells and eosinophils play a key role in several allergic reactions including asthma and anaphylaxis [84]. One of the postulated mechanisms of histamine toxicity is by stimulation of mast cells via signaling IgE and histamine receptor-1 (HR1) to release endogenous histamine and other cytotoxic mediators [36]. Mast cells have the ability to regulate the activities of numerous organs and tissues via releasing the variety of multifunctional preformed molecules, including histamine, proteases, prostanoids, heparin, and numerous cytokines, chemokines, growth factors, and lipid mediators [48]. The vascular endothelium can be significantly affected by these mediators, increasing the vascular permeability and adhesiveness. All the above-mentioned aspects had the ability to bring more inflammatory cells to the localized area causing further inflammation and tissue damage [6]. Moreover, eosinophils normally present in blood and other tissues such as skin, thymus, and spleen once activated by allergen (HIS) migrate to the site of inflammation. The eosinophil chemotactic factor produced by mast cells plays a significant role in bringing eosinophils to the inflamed area [61]. Eosinophils also secrete cytotoxic mediators as major basic proteins, cytokines, chemokines, lysosomal enzymes, growth factors, and ROS that induce inflammation and tissue necroptotic damage [25].

The inflammatory impact of HIS is confirmed by both immunohistochemical and molecular studies which determine a strong positive expression of the inflammatory markers Cox-2, TNF-α, IL-1β, and NF-κB. The vasodilation occurs during HIS-mediated inflammation results in both exudate and inflammatory cells accumulation in the interstitial tissues [22]. Additionally, HIS binds to H1R and H4R, causing generation of proinflammatory cytokines like IL-6 and TNF-α [87]. TNF-α, IL-1, and IL-6 are the crucial proinflammatory cytokines that

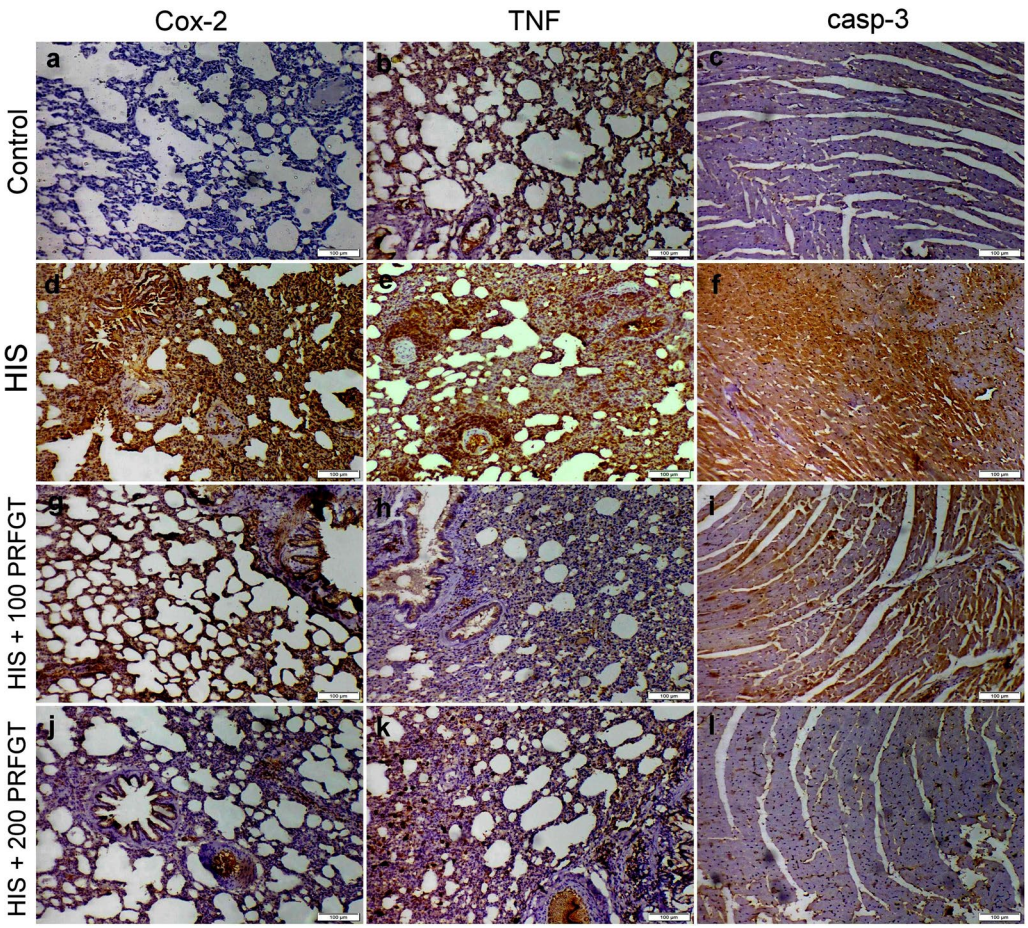

Fig. 5 Photomicrograph demonstrating the pulmonary expression of both Cox-2 and TNF-α immune markers as well as caspase-3 immunostaining in the heart sections of various groups. **a**–**c** Control group exhibited negative expression of the above-mentioned immune markers. **d**–**f** Group receiving HIS showed strong immunopositivity of Cox-2 and TNF-α in the pulmonary tissue along with strong caspase-3 protein expression in the myocardium. **g**–**i** Group receiving HIS + 100 mg PRFGT displayed moderate immunopositivity of Cox-2 and TNF-α in the pulmonary tissue along with negative caspase-3 protein expression in the myocardium. **j**–**l** Group receiving HIS + 200 mg PRFGT displayed negative expression of the studied immune markers in both lung and heart section

induce inflammation in many pulmonary pathologies and diseases. TNF-α is a cytokine that promotes inflammation and has a variety of biological consequences [92]. TNF-α induces infiltration of the inflammatory cells, production of inflammatory mediators, oxidative and nitrosative stress, airway hyperresponsiveness, and tissue remodeling [55]. The cyclooxygenase enzyme (Cox) is commonly linked to the incidence of many inflammatory disorders [91]. It has been demonstrated that proinflammatory cytokines can increase Cox-2, which exacerbates the inflammatory immune response in lung damage [38].

In the present investigation, we found that the Bax/casp-3 signaling pathway-mediated apoptosis also shared in the mechanism of cardiopulmonary toxicity that induced by HIS. Overproduction of ROS within cells damages proteins, nucleic acids, lipids, membranes, and organelles, which may trigger cell death processes including apoptosis [26]. Via the mitochondrial pathway, ROS can trigger the release of cytochrome c from the mitochondria and induce apoptosis [16]. In the presence of ATP, released cytochrome c interacts with apoptotic protease activating factor-1(Apaf-1) and activates caspase-9 to produce an apoptosome [9]. Caspases 3 and/or 7 are then activated by an active caspase-9, which cleaves a certain set of substrates and encourages cell death [42]. We found that HIS receiving groups showed strong immune expression of casp-3 along with upregulation of proto-oncogene genes c-fos, c-Myc, and c-Jun. These genes participate in cell cycle progression and cellular proliferation [100]. A regulatory protein called c-fos contains a basic leucine-zipper region that allows it to bind to a variety of proteins [101]. Both c-fos and c-Jun dimers promote the formation of the activator protein-1

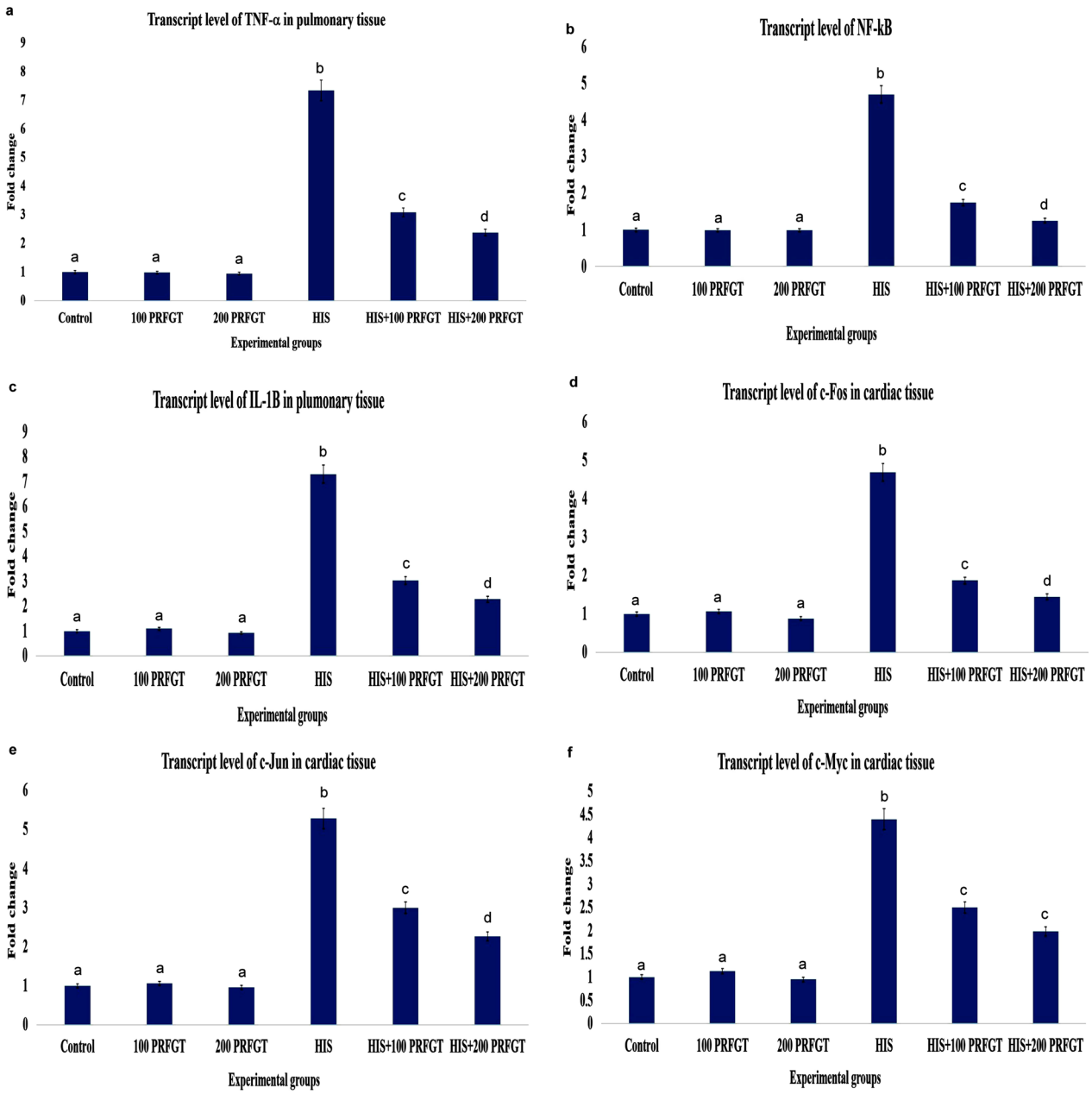

Fig. 6 Bar graphs display the variations in gene transcription levels between groups in lung and heart tissues. **a**, **b**, **c** Indicates m-RNA levels for the TNF-α, NF-κB, and IL-1β genes in pulmonary tissue. **d**, **e**, **f** m-RNA levels of c-Fos, c-Jun, and c-Myc genes respectively in the cardiac tissue. Means ± SEM are used to represent values ($n = 5$). Various superscript letters (a, b, c, etc.) indicate a significant difference between groups at $P \leq 0.05$

(AP-1) [40]. AP-1 regulates numerous biological functions, such as cell division, cell death, survival, and differentiation [102]. The c-fos gene aids in the process of myocardial apoptosis [11]. It is reported that c-Jun induces and transactivates *caspase-3* gene [83]. One of the most crucial transcriptional factors, c-MYC, controls a wide variety of cellular processes, including apoptosis, growth, and proliferation [62]. The ability of the c-Myc protein to promote apoptosis in a variety of cellular settings is one of its well-known functions [72].

Otherwise, the groups treated with PRFGT demonstrated a noticeable decrease in MDA levels and a higher antioxidant activity, indicating strong antioxidant properties of green tea phenolic-rich fraction. The presence of high concentration of flavonoids and phenolics may be primarily responsible for this action. Catechins present

in green tea are famous for their anti-inflammatory, antioxidant, cardioprotective, and anticancer effects. They are the elementary unit of compacted tannins generally recognized as pro-anthocyanidins with a variety of pharmaceutical functions [4, 5]. EGCG is the strongest antioxidant among all catechins in green tea [88]. EGCG acts as a scavenger of several ROS/RNS by capturing peroxyl radicals, and therefore, it can prevent membrane lipid peroxidation and protect cells from oxidative damage [77]. Gallic acid (GA) and its derivatives are considered the primary polyphenolic compounds in green tea and also in some fruits [63]. GA increases the levels of glutathione, glutathione peroxidase, glutathione reductase, and catalase as well as lowering the oxidative stress-related damage [56].

Our study showed that PRFGT decreased the expression of Cox-2 and TNF-α immune markers and downregulated the inflammatory genes (IL-1β, TNF-α, and NF-κB) in the pulmonary tissue, indicating the anti-inflammatory effect of green tea phenolic-rich fraction. One study revealed the ability GTE to reduce COX-2 activity, which attenuates lipid peroxidation and PGE2 accumulation [15]. Other studies explained the anti-inflammatory potential of green tea polyphenols by regulating the COX-2 and NF-κB pathways [67, 85, 94] investigated that EGCG-mediated NF-κB inactivation plays a key role in its anti-inflammatory potential via regulating Cox-2 and iNOS. Green tea polyphenols exert powerful antioxidant and anti-inflammatory effects by regulating a variety of gene expressions, including Nrf2, Cox-2, iNOS, NF-κB, AP-1, and STATs [89]. Previous in vitro investigation has shown that EGCG has anti-inflammatory properties and prevented neutrophil chemotaxis [8]. Numerous studies have demonstrated that EGCG reduces inflammation by altering the NF-κB/AP-1 pathway [99]. For instance, the release of histamine and leukotriene B4 was significantly inhibited by EGCG [59]. More studies discussed the anti-inflammatory effect of GA against several pulmonary hypersensitivity reactions which may be mediated by inactivating the transcription levels of IL-33, IL-5, and IL-13 [75, 93]. Recent study proved the anti-inflammatory effects of GA against toxic hepatitis via downregulating the proinflammatory cytokines, IL-1, IL-6, Cox-2, TNF-α [65]. Additionally, our study revealed that PRFGT showed mild expression of caspase-3 immune marker in myocardial tissue along with down-regulation of apoptotic genes such as c-fos, c-Myc, and c-Jun which indicates the strong anti-apoptotic effect of green tea extracted fractions. This outcome agreed with the findings of Zong et al. [103], who showed that EGCG had an anti-apoptotic potential. Moreover, some studies showed that EGCG has a cardioprotective effect via significant reduction in the pro-apoptotic proteins such as Bax, caspase-9, and caspase-3 and increases the anti-apoptotic proteins such as Bcl2 [66]. Another study showed that the treatment with EGCG results in mitochondrial-level cardiac protection via reversed the mitochondrial and nuclear changes caused by apoptosis [3]. Furthermore, GA had a potent anti-apoptotic activity through inhibition of Bax/Bcl2 ratio [14, 53] and reduction of the levels of caspase-3 [57].

5 Conclusion

We concluded that the weekly oral intake of HIS to rats had the ability to cause severe cardiopulmonary toxicity either through oxido-inflammatory stress or apoptosis. Additionally, we found that the cotreatment of PRFGT with HIS can restore the oxidant/antioxidant balance and improve the microscopic picture of both lung and heart tissues. PRFGT had an anti-inflammatory effect via modulating Cox-2/NF-κB mediated by inactivation of proinflammatory cytokines including TNF-α and IL-1β. Furthermore, the anti-apoptotic effect of PRFGT is attributed to downregulating the casp-3, c-jun, c-fos, and c-myc genes. We found that PRFGT has a synergistic effect aid in the prevention of HIS-inducing cardiopulmonary toxicity suggesting its therapeutic potential against several HIS-mediated inflammatory diseases like atopic dermatitis, neuroinflammation, and allergies. We recommend daily intake of green tea as a beverage or adding it to foods containing elevated levels of HIS to prevent its possible toxicity.

Abbreviations

casp-3	Caspase-3
CAT	Catalase
c-Fos	Fos proto-oncogene, AP-1 transcription factor subunit
c-Jun	C-Jun *N*-terminal kinases (JNKs)
c-Myc	C-myelocytomatosis oncogene product or Myc proto-oncogene, bHLH transcription factor
Cox-2	Cyclooxygenase
DAO	Diamine oxidase
GAPDH	Glyceraldehyde3-phosphate dehydrogenase
GSH	Reduced glutathione
GTE	Green tea extract
HIS	Histamine
HNMT	Histamine *N*-methyltransferase
HR	Histamine receptor
IL-1β	Interleukin-1 beta
LPO	Lipid peroxidation
MDA	Malondialdehyde
NF-κB	Nuclear factor kappa-B
PRFGT	Phenolic-rich fraction of green tea
ROS	Reactive oxygen species
TNF-α	Tumor necrosis factor alpha

Acknowledgements

Not applicable.

Author contributions

EIH, WAM, HAM, and MAM contributed to research concept; MYI extracted preparation and identification; EIH and WAM were involved in experiment and sampling; EIH, WAM, and MAM contributed to pathological and

immunohistochemical evaluation; SK and WAM were involved in oxidative stress markers and gene expression analysis; EIH, WAM, HAM, and MAM drafted the manuscript; and all authors contributed to revision and final approval of this version for publication.

Funding
This research did not receive any specific grant from funding agencies in the public, commercial, or not-for-profit sectors.

Availability of data and materials
All data generated or analyzed during this study are included in this published article.

Declarations

Ethics approval and consent to participate
All Institutional and National Guidelines for the care and use of animals were followed.

Consent for publication
Not applicable.

Competing interests
No competing interests declared.

Author details
[1]Pathology Department, Faculty of Veterinary Medicine, Cairo University, P.O. Box 12211, Giza, Egypt. [2]Department of Biochemistry and Molecular Biology, Faculty of Veterinary Medicine, Cairo University, Giza 12211, Egypt. [3]Department of Pharmacognosy, Faculty of Pharmacy, Cairo University, Giza 12211, Egypt. [4]Department of Food Hygiene and Control, Faculty of Veterinary Medicine, Cairo University, Giza 12211, Egypt.

Received: 4 September 2023 Accepted: 5 January 2024
Published online: 12 January 2024

References

1. Abu-Reidah IM, Arráez-Román D, Lozano-Sánchez J, Segura-Carretero A, Fernández-Gutiérrez A (2013) Phytochemical characterisation of green beans (*Phaseolus vulgaris* L.) by using high-performance liquid chromatography coupled with time-of-flight mass spectrometry. Phytochem Anal 24(2):105–116
2. Abu-Reidah IM, del Mar Contreras M, Arráez-Román D, Fernández-Gutiérrez A, Segura-Carretero A (2014) UHPLC-ESI-QTOF-MS-based metabolic profiling of *Vicia faba* L. (Fabaceae) seeds as a key strategy for characterization in foodomics. Electrophoresis 35(11):1571–1581
3. Adikesavan G, Vinayagam MM, Abdulrahman LA, Chinnasamy T (2013) Epigallocatechin-gallate (EGCG) stabilizes the mitochondrial enzymes and inhibits the apoptosis in cigarette smoke-induced myocardial dysfunction in rats. Mol Biol Rep 40(12):6533–6545
4. Ali A, Cottrell JJ, Dunshea FR (2022) LC-MS/MS characterization of phenolic metabolites and their antioxidant activities from Australian Native Plants. Metabolites 12(11):1016
5. Ali WA, Moselhy WA, Ibrahim MA, Amin MM, Kamel S, Eldomany EB (2022) Protective effect of rutin and β-cyclodextrin against hepatotoxicity and nephrotoxicity induced by lambda-cyhalothrin in Wistar rats: biochemical, pathological indices and molecular analysis. Biomarkers 27(7):625–636. https://doi.org/10.1080/1354750X.2022.2087003
6. Amin K (2012) The role of mast cells in allergic inflammation. Respir Med 106(1):9–14
7. Atiakshin D, Samoilova V, Buchwalow I, Boecker W, Tiemann M (2017) Characterization of mast cell populations using different methods for their identification. Histochem Cell Biol 147(6):683–694
8. Bae HB, Li M, Kim JP, Kim SJ, Jeong CW, Lee HG, Kim WM, Kim HS, Kwak SH (2010) The effect of epigallocatechin gallate on lipopolysaccharide-induced acute lung injury in a murine model. Inflammation 33:82–91. https://doi.org/10.1007/s10753-009-9161-z
9. Bakhshoudeh M, Mehdizadeh K, Hosseinkhani S, Ataei F (2021) Upregulation of apoptotic protease activating factor-1 expression correlates with anti-tumor effect of taxane drug. Med Oncol 38(8):1–11
10. Bancroft JD, Gamble M (2013) Theories and practice of histological techniques, 6th edn. Churchil Livingstone, New York
11. Bao Y, Qiao Y, Yu H, Zhang Z, Yang H, Xin X, Chen Y, Guo Y, Wu N, Jia D (2021) miRNA-27a transcription activated by c-Fos regulates myocardial ischemia-reperfusion injury by targeting ATAD3a. Oxid Med Cell Longev 2021:1–16
12. Berman RL (2020) Afghanistan desert particulate matter promotes inflammatory signaling and airway hyperresponsiveness. University of Colorado Denver, Anschutz Medical Campus, Denver
13. Cai J, Jing D, Shi M, Liu Y, Lin T, Xie Z, Zhu Y, Zhao H, Shi X, Du F, Zhao G (2014) Epigallocatechin gallate (EGCG) attenuates infrasound-induced neuronal impairment by inhibiting microglia-mediated inflammation. J Nutr Biochem 25(7):716–725
14. Chandrasekhar Y, Phani Kumar G, Ramya EM, Anilakumar KR (2018) Gallic acid protects 6-OHDA induced neurotoxicity by attenuating oxidative stress in human dopaminergic cell line. Neurochem Res 43(6):1150–1160
15. Chung MY, Mah E, Masterjohn C, Noh SK, Park HJ, Clark RM, Park YK, Lee JY, Bruno RS (2015) Green tea lowers hepatic COX-2 and prostaglandin E2 in rats with dietary fat-induced nonalcoholic steatohepatitis. J Med Food 18(6):648–655
16. Circu ML, Aw TY (2012) Glutathione and modulation of cell apoptosis. Biochim Biophys Acta Mol Cell Res 1823(10):1767–1777
17. Comas-Basté O, Sánchez-Pérez S, Veciana-Nogués MT, Latorre-Moratalla M, Vidal-Carou MDC (2020) Histamine intolerance: the current state of the art. Biomolecules 10(8):1181
18. Crowley SD (2014) The cooperative roles of inflammation and oxidative stress in the pathogenesis of hypertension. Antioxid Redox Signal 20(1):102–120
19. Eldanasory OA, Eljaaly K, Memish ZA, Al-Tawfiq JA (2020) Histamine release theory and roles of antihistamine in the treatment of cytokines storm of COVID-19. Travel Med Infect Disease 37:101874
20. Elleithy EMM, Bawish BM, Kamel S, Ismael E, Bashir DW, Hamza D, Fahmy KNE (2023) Influence of dietary Bacillus coagulans and/or Bacillus licheniformis-based probiotics on performance, gut health, gene expression, and litter quality of broiler chickens. Trop Anim Health Prod 55(1):38. https://doi.org/10.1007/s11250-023-03453-2
21. Ellis LZ, Liu W, Luo Y, Okamoto M, Qu D, Dunn JH, Fujita M (2011) Green tea polyphenol epigallocatechin-3-gallate suppresses melanoma growth by inhibiting inflammasome and IL-1β secretion. Biochem Biophys Res Commun 414(3):551–556
22. Ely MR, Ratchford SM, La Salle DT, Trinity JD, Wray DW, Halliwill JR (2020) Effect of histamine-receptor antagonism on leg blood flow during exercise. J Appl Physiol 128(6):1626–1634
23. Ezzat MI, Issa MY, Sallam IE, Zaafar D, Khalil HM, Mousa MR, Sabry D, Gawish AY, Elghandour AH, Mohsen E (2022) Impact of different processing methods on the phenolics and neuroprotective activity of *Fragaria ananassa* Duch. extracts in ad-galactose and aluminum chloride-induced rat model of aging. Food Funct 13(14):7794–7812
24. Faustino-Rocha AI, Ferreira R, Gama A, Oliveira PA, Ginja M (2017) Antihistamines as promising drugs in cancer therapy. Life Sci 172:27–41
25. George L, Brightling CE (2016) Eosinophilic airway inflammation: role in asthma and chronic obstructive pulmonary disease. Ther Adv Chronic Disease 7(1):34–51
26. Halliwell B (2011) Free radicals and antioxidants–quovadis? Trends Pharmacol Sci 32(3):125–130
27. Han Z, Wen M, Zhang H, Zhang L, Wan X, Ho CT (2022) LC-MS based metabolomics and sensory evaluation reveal the critical compounds of different grades of Huangshan Maofeng green tea. Food Chem 374:131796
28. Hashempur MH, Sadrneshin S, Mosavat SH, Ashraf A (2018) Green tea (*Camellia sinensis*) for patients with knee osteoarthritis: a randomized open-label active-controlled clinical trial. Clin Nutr 37(1):85–90
29. Hassanain E, Silverberg JI, Norowitz KB, Chice S, Bluth MH, Brody N, Joks R, Durkin HG, Smith-Norowitz TA (2010) Green tea (*Camellia sinensis*) suppresses B cell production of IgE without inducing apoptosis. Ann Clin Lab Sci 40(2):135–143

30. Hassanen EI, Kamel S, Mohamed WA, Mansour HA, Mahmoud MA (2023) The potential mechanism of histamine-inducing cardiopulmonary inflammation and apoptosis in a novel oral model of rat intoxication. Toxicology 484:153410
31. Hassanen EI, Tohamy AF, Issa MY, Ibrahim MA, Farroh KY, Hassan AM (2019). Pomegranate juice diminishes the mitochondria-dependent cell death and NF-kB signaling pathway induced by copper oxide nanoparticles on liver and kidneys of rats. Int J Nanomed 8905–8922
32. Hassanen EI, Abdelrahman RE, Aboul-Ella H, El-Dek S, Shaalan M (2023) Mechanistic approach to the pulmonary Oxido-inflammatory stress induced by cobalt ferrite nanoparticles in rats. Biol Trace Elem Res. https://doi.org/10.1007/s12011-023-03700-5
33. He G, Hou X, Han M, Qiu S, Li Y, Qin S, Chen X (2022) Discrimination and polyphenol compositions of green teas with seasonal variations based on UPLC-QTOF/MS combined with chemometrics. J Food Compos Anal 105:104267
34. Heinrich U, Moore CE, De Spirt S, Tronnier H, Stahl W (2011) Green tea polyphenols provide photoprotection, increase microcirculation, and modulate skin properties of women. J Nutr 141(6):1202–1208
35. Hungerford JM (2010) Scombroid poisoning: a review. Toxicon 56(2):231–243
36. Hungerford JM (2021) Histamine and scombrotoxins. Toxicon 201:115–126
37. Ibrahim MA, Radwan MI, Kim HK, Han J, Warda M (2020) Evaluation of global expression of selected genes as potential candidates for internal normalizing control during transcriptome analysis in dromedary camel (*Camelus dromedarius*). Small Ruminant Res 184:106050. https://doi.org/10.1016/j.smallrumres.2020.106050
38. Jakubowski A, Maksimovich N, Olszanecki R, Gebska A, Gasser H, Podesser BK, Hallström S, Chlopicki S (2009) S-nitroso human serum albumin given after LPS challenge reduces acute lung injury and prolongs survival in a rat model of endotoxemia. Naunyn-Schmiedeberg's Arch Pharmacol 379(3):281–290. https://doi.org/10.1007/s00210-008-0351-2
39. Jeszka-Skowron M, Zgoła-Grześkowiak A, Frankowski R (2018) *Cistus incanus* a promising herbal tea rich in bioactive compounds: LC–MS/MS determination of catechins, flavonols, phenolic acids and alkaloids—a comparison with *Camellia sinensis*, Rooibos and Hoan Ngoc herbal tea. J Food Compos Anal 74:71–81
40. Jin SP, Kim JH, Kim MA, Yang HK, Lee HE, Lee HS, Kim WH (2007) Prognostic significance of loss of c-fos protein in gastric carcinoma. Pathol Oncol Res 13(4):284–289
41. Kamel S, Ibrahim MA, Awad ET, El-Hindi HMA, Abdel-Aziz SA (2018) Molecular cloning and characterization of the novel CYP2J2 in dromedary camels (*Camelus dromedarius*). Int J Biol Macromol 120:1770–1776
42. Karimzadeh S, Hosseinkhani S, Fathi A, Ataei F, Baharvand H (2018) Insufficient Apaf-1 expression in early stages of neural differentiation of human embryonic stem cells might protect them from apoptosis. Eur J Cell Biol 97(2):126–135
43. Kasas AHE, Farag IM, Darwish HR, Soliman YA, Nagar EME, Ibrahim MA, Kamel S, Warda M (2022) Molecular characterization of alpha subunit 1 of sodium pump (ATP1A1) gene in *Camelus dromedarius*: its differential tissue expression potentially interprets the role in osmoregulation. Mol Biol Rep 49(5):3849–3861
44. Kaya Z, Yayla M, Cinar I, Atila NE, Ozmen S, Bayraktutan Z, Bilici D (2019) Epigallocatechin-3-gallate (EGCG) exerts therapeutic effect on acute inflammatory otitis media in rats. Int J Pediatr Otorhinolaryngol 124:106–110
45. Kelebek H (2016) LC-DAD–ESI-MS/MS characterization of phenolic constituents in Turkish black tea: effect of infusion time and temperature. Food Chem 204:227–238
46. Khan G, Haque SE, Anwer T, Ahsan MN, Safhi MM, Alam MF (2014) Cardioprotective effect of green tea extract on doxorubicin-induced cardiotoxicity in rats. Acta Pol Pharm 71(5):861–868
47. Kim SH, Jun CD, Suk K, Choi BJ, Lim H, Park S, Lee SH, Shin HY, Kim DK, Shin TY (2006) Gallic acid inhibits histamine release and pro-inflammatory cytokine production in mast cells. Toxicol Sci 91:123–131
48. Krystel-Whittemore M, Dileepan KN, Wood JG (2016) Mast cell: a multi-functional master cell. Front Immunol 620
49. Lambert JD, Elias RJ (2010) The antioxidant and pro-oxidant activities of green tea polyphenols: a role in cancer prevention. Arch Biochem Biophys 501(1):65–72
50. Lamoral-Theys D, Pottier L, Dufrasne F, Neve J, Dubois J, Kornienko A, Kiss R, Ingrassia L (2010) Natural polyphenols display anticancer properties through inhibition of kinase activity. Curr Med Chem 17(9):812–825
51. Li M, Kelly BT, Hagerman AE (2016) Isolation of Epigallocatechin from Green Tea Extract by Means of Immobilized Tannase. Planta Med Int Open 3(02):e35–e38
52. Lieberman P (2011) The basics of histamine biology. Ann Allergy, Asthma Immunol 106(2):S2–S5
53. Lin MC, Yin MC (2013) Preventive effects of ellagic acid against doxorubicin-induced cardiotoxicity in mice. Cardiovasc Toxicol 13(3):185–193
54. Liu Y, Huang W, Zhang C, Li C, Fang Z, Zeng Z, Hu B, Chen H, Wu W, Wang T, Lan X (2022) Targeted and untargeted metabolomic analyses and biological activity of Tibetan tea. Food Chem 384:132517
55. Malaviya R, Laskin JD, Laskin DL (2017) Anti-TNFα therapy in inflammatory lung diseases. Pharmacol Ther 180:90–98
56. Mansouri MT, Farbood Y, Sameri MJ, Sarkaki A, Naghizadeh B, Rafeirad M (2013) Neuroprotective effects of oral gallic acid against oxidative stress induced by 6-hydroxydopamine in rats. Food Chem 138(2–3):1028–1033
57. Mard SA, Mojadami S, Farbood Y, Gharib Naseri MK (2015) The anti-inflammatory and anti-apoptotic effects of gallic acid against mucosal inflammation- and erosions-induced by gastric ischemia-reperfusion in rats. Vet Res forum Int Q J 6(4):305–311
58. Massari NA, Nicoud MB, Medina VA (2020) Histamine receptors and cancer pharmacology: an update. Br J Pharmacol 177(3):516–538
59. Mokra D, Adamcakova J, Mokry J (2022) Green tea polyphenol (-)-epigallocatechin-3-gallate (EGCG): a time for a new player in the treatment of respiratory diseases? Antioxidants 11(8):1566
60. Mohamed WA, Hassanen EI, Mansour HA, Mahmoud MA (2023) Immunohistochemical evaluation of histamine levels and hygienic aspect of little tunny (*Euthynnus alletteratus*) musculature at different environment time and temperature. J Aquat Food Product Technol 32:637–653
61. Nash AA, Dalziel RG, Fitzgerald JR (2015) Mechanisms of cell and tissue damage. Mims' Pathog Infect Disease 171
62. Nguyen L, Papenhausen P, Shao H (2017) The role of c-MYC in B-cell lymphomas: diagnostic and molecular aspects. Genes 8(4):116
63. Nikbakht J, Hemmati AA, Arzi A, Mansouri MT, Rezaie A, Ghafourian M (2015) Protective effect of gallic acid against bleomycin-induced pulmonary fibrosis in rats. Pharmacol Rep 67(6):1061–1067
64. Ohishi T, Goto S, Monira P, Isemura M, Nakamura Y (2016) Anti-inflammatory action of green tea. Anti-Inflamm Anti-Allergy Agents Med Chem 15(2):74–90
65. Ojeaburu SI, Oriakhi K (2021) Hepatoprotective, antioxidant and anti-inflammatory potentials of gallic acid in carbon tetrachloride-induced hepatic damage in Wistar rats. Toxicol Rep 8:177–185
66. Othman AI, Elkomy MM, El-Missiry MA, Dardor M (2017) Epigallocatechin-3-gallate prevents cardiac apoptosis by modulating the intrinsic apoptotic pathway in isoproterenol-induced myocardial infarction. Eur J Pharmacol 794:27–36
67. Oz HS, Chen TS (2008) Green-tea polyphenols downregulate cyclooxygenase and Bcl-2 activity in acetaminophen-induced hepatotoxicity. Dig Dis Sci 53:2980–2988
68. Panula P, Chazot PL, Cowart M, Gutzmer R, Leurs R, Liu WL, Stark H, Thurmond RL, Haas HL (2015) International union of basic and clinical pharmacology. XCVIII. Histamine receptors. Pharmacol Rev 67(3):601–655
69. Passmore MR, Byrne L, Obonyo NG, See Hoe LE, Boon AC, Diab SD, Dunster KR, Bisht K, Tung JP, Fauzi MH, Narula M (2018) Inflammation and lung injury in an ovine model of fluid resuscitated endotoxemic shock. Respirat Res 19(1):1–10
70. Pawankar R, Canonica GW, Holgate ST, Lockey RF, Blaiss MS (2011) WAO white book on allergy. Milwaukee WI World Allergy Organ 3:156–157
71. Pawankar R (2014) Allergic diseases and asthma: a global public health concern and a call to action. World Allergy Organ J 7(1):12. https://doi.org/10.1186/1939-4551-7-12)
72. Phesse TJ, Myant KB, Cole AM, Ridgway RA, Pearson H, Muncan V, Van Den Brink GR, Vousden KH, Sears R, Vassilev LT, Clarke AR (2014) Endogenous c-Myc is essential for p53-induced apoptosis in response to DNA damage in vivo. Cell Death Differ 21(6):956–966

73. Razavi SM, Deyhimi P, Homayouni S (2015) Comparative evaluation of eosinophils in normal mucosa, dysplastic mucosa and oral squamous cell carcinoma with hematoxylin-eosin, Congo red, and EMR1 immunohistochemical staining techniques. Electr Phys 7(2):1019
74. Relja B, Töttel E, Breig L, Henrich D, Schneider H, Marzi I, Lehnert M (2012) Plant polyphenols attenuate hepatic injury after hemorrhage/resuscitation by inhibition of apoptosis, oxidative stress, and inflammation via NF-kappaB in rats. Eur J Nutr 51:311–321
75. Rong Y, Cao B, Liu B, Li W, Chen Y, Chen H, Liu Y, Liu T (2018) A novel Gallic acid derivative attenuates BLM-induced pulmonary fibrosis in mice. Int Immunopharmacol 64:183–191
76. Schwelberger HG (2009) Histamine intolerance: overestimated or underestimated? Inflamm Res 58:51
77. Shanmugam T, Selvaraj M, Poomalai S (2016) Epigallocatechin gallate potentially abrogates fluoride induced lung oxidative stress, inflammation via Nrf2/Keap1 signaling pathway in rats: an in-vivo and in-silico study. Int Immunopharmacol 39:128–139
78. Shen CL, Samathanam C, Graham S, Dagda RY, Chyu MC, Dunn DM (2012) Green tea polyphenols and 1-α-OH-vitamin D3 attenuate chronic inflammation-induced myocardial fibrosis in female rats. J Med Food 15(3):269–277
79. Shen CL, Yeh JK, Samathanam C, Cao JJ, Stoecker BJ, Dagda RY, Chyu MC, Wang JS (2011) Protective actions of green tea polyphenols and alfacalcidol on bone microstructure in female rats with chronic inflammation. J Nutrit Biochem 22(7):673–680
80. Shevchuk A, Jayasinghe L, Kuhnert N (2018) Differentiation of black tea infusions according to origin, processing and botanical varieties using multivariate statistical analysis of LC-MS data. Food Res Int 109:387–402
81. Shulpekova YO, Nechaev VM, Popova IR, Deeva TA, Kopylov AT, Malsagova KA, Kaysheva AL, Ivashkin VT (2021) Food intolerance: the role of histamine. Nutrients 13(9):3207
82. Singh R, Akhtar N, Haqqi TM (2010) Green tea polyphenol epigallocatechi3-gallate: inflammation and arthritis. Life Sci 86(25–26):907–918
83. Song B, Xie B, Wang C, Li M (2011) Caspase-3 is a target gene of c-Jun: ATF2 heterodimers during apoptosis induced by activity deprivation in cerebellar granule neurons. Neurosci Lett 505(2):76–81
84. Stone KD, Prussin C, Metcalfe DD (2010) IgE, mast cells, basophils, and eosinophils. J Allergy Clin Immunol 125(2):S73–S80
85. Surh YJ, Chun KS, Cha HH, Han SS, Keum YS, Park KK, Lee SS (2001) Molecular mechanisms underlying chemopreventive activities of anti-inflammatory phytochemicals: down-regulation of COX-2 and iNOS through suppression of NF-κB activation. Mutation Res Fund Mol Mech Mutagen 480:243–268
86. Tachibana H, Sunada Y, Miyase T, Sano M, Maeda-Yamamoto M, Yamada K (2000) Identification of a methylated tea catechin as an inhibitor of degranulation in human basophilic KU812 cells. Biosci Biotechnol Biochem 64:452–454
87. Thangam EB, Jemima EA, Singh H, Baig MS, Khan M, Mathias CB, Church MK, Saluja R (2018) The role of histamine and histamine receptors in mast cell-mediated allergy and inflammation: the hunt for new therapeutic targets. Front Immunol 9:1873
88. Thangapandiyan S, Miltonprabu S (2013) Epigallocatechin gallate effectively ameliorates fluoride-induced oxidative stress and DNA damage in the liver of rats. Can J Physiol Pharmacol 91(7):528–537
89. Truong VL, Jeong WS (2022) Antioxidant and anti-inflammatory roles of tea polyphenols in inflammatory bowel diseases. Food Sci Hum Wellness 11(3):502–511
90. Wang J, Huang J, Wang L, Chen C, Yang D, Jin M, Bai C, Song Y (2017) Urban particulate matter triggers lung inflammation via the ROS-MAPK-NF-κB signaling pathway. J Thorac Dis 9(11):4398
91. Wang J, Liu YT, Xiao L, Zhu L, Wang Q, Yan T (2014) Anti-inflammatory effects of apigenin in lipopolysaccharide-induced inflammatory in acute lung injury by suppressing COX-2 and NF-kB pathway. Inflammation 37(6):2085–2090
92. Wang T, He C (2018) Pro-inflammatory cytokines: the link between obesity and osteoarthritis. Cytokine Growth Factor Rev 44:38–50
93. Wang X, Zhao H, Ma C, Lv L, Feng J, Han S (2018) Gallic acid attenuates allergic airway inflammation via suppressed interleukin-33 and group 2 innate lymphoid cells in ovalbumin-induced asthma in mice. Int Forum Allergy Rhinol 8(11):1284–1290
94. Wang D, Zhang M, Wang T, Cai M, Qian F, Sun Y, Wang Y (2019) Green tea polyphenols prevent lipopolysaccharide-induced inflammatory liver injury in mice by inhibiting NLRP3 inflammasome activation. Food Funct 10(7):3898–3908
95. Wen M, Zhou F, Zhu M, Han Z, Lai G, Jiang Z, Long P, Zhang L (2023) Monitoring of pickled tea during processing: from LC-MS based metabolomics analysis to inhibitory activities on α-amylase and α-glycosidase. J Food Compos Anal 117:105108
96. Worm J, Falkenberg K, Olesen J (2019) Histamine and migraine revisited: mechanisms and possible drug targets. J Headache Pain 20(1):1–12
97. Wu SY, Silverberg JI, Joks R, Durkin HG, Smith-Norowitz TA (2012) Green tea (*Camelia sinensis*) mediated suppression of IgE production by peripheral blood mononuclear cells of allergic asthmatic humans. Scand J Immunol 76(3):306–310
98. Xu Y, Zhang JJ, Xiong L, Zhang L, Sun D, Liu H (2010) Green tea polyphenols inhibit cognitive impairment induced by chronic cerebral hypoperfusion via modulating oxidative stress. J Nutr Biochem 21(8):741–748
99. Yoon JY, Kwon HH, Min SU, Thiboutot DM, Suh DH (2013) Epigallocatechin-3-gallate improves acne in humans by modulating intracellular molecular targets and inhibiting *P. acnes*. J Investig Dermatol 133(2):429–440
100. Yuen MF, Wu PC, Lai VCH, Lau JYN, Lai CL (2001) Expression of c-Myc, c-Fos, and c-jun in hepatocellular carcinoma. Cancer 91(1):106–112
101. Zhang S, Zhang M, Goldstein S, Li Y, Ge J, He B, Ruiz G (2013) The effect of c-fos on acute myocardial infarction and the significance of metoprolol intervention in a rat model. Cell Biochem Biophys 65(2):249–255
102. Zhou H, Gao J, Lu ZY, Lu L, Dai W, Xu M (2007) Role of c-Fos/JunD in protecting stress-induced cell death. Cell Prolif 40(3):431–444
103. Zong Y, Chen F, Li S, Zhang H (2021) Epigallocatechin-3-gallate (EGCG) prevents aminoglycosides-induced ototoxicity via anti-oxidative and anti-apoptotic pathways. Int J Pediatr Otorhinolaryngol 150:110920

Publisher's Note